Eur. Phys. J. D **12**, 53–59 (2000)

THE EUROPEAN PHYSICAL JOURNAL D

EDP Sciences

Line-shape of dark line and maser emission profile in CPT

F. Levi[1,a], A. Godone[1], J. Vanier[2,b], S. Micalizio[3,c], and G. Modugno[4,d]

[1] Istituto elettrotecnico Nazionale "G. Ferraris", Str. delle Cacce 91, 10135 Torino, Italy
[2] Département de Physique, Université de Montréal, Montréal, QUE, Canada
[3] Politecnico di Torino, C.so duca degli Abruzzi 27, Torino, Italy
[4] Università di Firenze, LENS, Largo E. Fermi 2, Firenze, Italy

Received 3 March 2000 and Received in final form 10 April 2000

Abstract. The paper is concerned with the line shapes of resonance phenomena observed in Coherent Population Trapping (CPT) applied to alkali atoms in a cell containing a buffer gas. Significant asymmetries and departures from a Lorentzian shape have been observed in connection with the measurement of dark lines and CPT maser emission profiles. Measurements are reported as a function of the power and frequency tuning of the laser used to create the CPT phenomenon. The paper reports on different experimental conditions and a comparison between theory and experiments is made for the cases of cesium and rubidium in a buffer gas.

PACS. 32.70.Jz Line shapes, widths, and shifts – 42.50.Gy Effects of atomic coherence on propagation, absorption, and amplification of light

1 Introduction

In recent years, the possibility of using atomic three level systems to realize a new generation of atomic frequency standards [1–3] or other measurement instruments such as magnetometers [4] has been proposed by several groups. In the practical implementation of a high resolution atomic reference, all the effects that may lead to shifts or asymmetries of the resonance line shape are of crucial importance. In this paper we analyze, both theoretically and experimentally, several effects that may affect the atomic response to a Λ excitation scheme.

The observation of a Λ transition in an alkali metal vapor cell containing a buffer gas is a straightforward experiment. In fact, the first sidebands of a single laser modulated at half the hyperfine transition frequency are sufficient to excite the Λ transition and to produce a coherent superposition of the atomic ground states (Coherent Population Trapping or CPT). When the coherence is established, two main effects appear: a dark line in the fluorescence spectrum (an Electromagnetically Induced Transparency effect) [5], and coherent microwave emission due to the hyperfine coherence created in the ground state, when the ensemble is placed in a microwave cavity (CPT-maser) [6].

The theory of these systems has been widely examined [7–9]. In the present article, we will recall first some theoretical results in order to go into a more detailed theoretical analysis of the line-shape. In particular, the effect of the laser beam profile and of the asymmetries of the excitation process on the line-shape will be considered and compared with the experimental results.

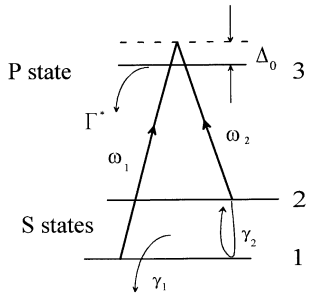

Fig. 1. Three level scheme representing the Λ transition in alkali atoms: in Cs the hyperfine frequency is 9.2 GHz and the optical wavelength (D_2 line) is 852 nm; in ^{87}Rb the hyperfine frequency is 6.8 GHz and the optical wavelength are (D_1 line) 795 nm and (D_2 line) 780 nm; typical values of the relaxation parameters are: $\Gamma^*/2\pi \approx 700$ MHz and $\gamma_1 \approx \gamma_2 \approx 500$ s^{-1}.

2 Theory

The evolution of the three level system shown in Figure 1 is analyzed in the ensemble averaged density matrix formalism. Starting from the theory developed in [8], we have

[a] e-mail: Levi@tf.ien.it
[b] e-mail: jacques.vanier@sympatico.ca
[c] e-mail: Micali@tf.ien.it
[d] e-mail: modugno@aix6.sns.it

(with minor changes in notation):

$$\begin{cases} \rho_{11} + \rho_{22} \approx 1 \\ \dot{\rho}_{33} + \Gamma^* \rho_{33} = -\omega_{\mathrm{R}1} \operatorname{Im} \delta_{13} - \omega_{\mathrm{R}2} \operatorname{Im} \delta_{23} \\ \dot{\Delta} + \gamma_1 \Delta = +\omega_{\mathrm{R}2} \operatorname{Im} \delta_{23} - \omega_{\mathrm{R}1} \operatorname{Im} \delta_{13} \\ \dot{\delta}_{12} + (\gamma_2 + \mathrm{i}\Omega_\mu)\delta_{12} = +\mathrm{i}\dfrac{\omega_{\mathrm{R}1}}{2}\delta_{32} - \mathrm{i}\dfrac{\omega_{\mathrm{R}2}}{2}\delta_{13} \\ \dot{\delta}_{13} + \left(\dfrac{1}{2}\Gamma^* + \mathrm{i}\Delta_0\right)\delta_{13} = -\mathrm{i}\dfrac{\omega_{\mathrm{R}1}}{4}(1 - \Delta) - \mathrm{i}\dfrac{\omega_{\mathrm{R}2}}{2}\delta_{12} \\ \dot{\delta}_{23} + \left(\dfrac{1}{2}\Gamma^* + \mathrm{i}\Delta_0\right)\delta_{23} = -\mathrm{i}\dfrac{\omega_{\mathrm{R}2}}{4}(1 + \Delta) - \mathrm{i}\dfrac{\omega_{\mathrm{R}1}}{2}\delta_{12}^* \end{cases} \tag{1}$$

where the various terms are defined as follows: Δ is the population difference in the ground states ($\Delta = \rho_{22} - \rho_{11}$), $\omega_{\mathrm{R}1}$ and $\omega_{\mathrm{R}2}$ are the Rabi frequencies of the optical transitions, Γ^* is the lifetime of the excited state taking into account all the relaxation processes (spontaneous decay, collisions with the buffer gas, etc.), γ_1 and γ_2 are respectively the population inversion and the coherence relaxation rates, Ω_μ is the detuning between the laser radiation difference and the hyperfine transition frequency and Δ_0 is the detuning of the laser carrier from the optical line "center of gravity". The off diagonal terms of the density matrix (coherences) have been assumed to have the form:

$$\begin{cases} \rho_{12} = \delta_{12}\, \mathrm{e}^{\mathrm{i}(\omega_1 - \omega_2)t} \\ \rho_{13} = \delta_{13}\, \mathrm{e}^{\mathrm{i}\omega_1 t} \\ \rho_{23} = \delta_{23}\, \mathrm{e}^{\mathrm{i}\omega_2 t} \end{cases}. \tag{2}$$

The following physical assumptions have been made to obtain the system of equations (1):

(1) the saturation of the optical transitions is small, $\omega_{\mathrm{R}1}$, $\omega_{\mathrm{R}2} \ll \Gamma^*$;
(2) the Rabi frequency of the generated microwave field is small compared to the atomic line width and its effect on the system can be neglected[1];
(3) the microwave detuning is small compared to the optical line width.

The case when the two Rabi frequencies are equal, ($\omega_{\mathrm{R}1} = \omega_{\mathrm{R}2} = \omega_{\mathrm{R}}$) was discussed in details in [8]. The main results reported in that article with respect to the population in the excited state and the coherence in the ground state are summarized below.

The optical fluorescence is directly proportional to the population in the excited state ρ_{33}. Solving system (1) in the stationary condition ($\partial/\partial t = 0$) we have:

$$\rho_{33} = \left(\frac{\omega_{\mathrm{R}}}{\Gamma^*}\right)^2 \left(1 - \frac{\omega_{\mathrm{R}}^2}{\Gamma^*} \frac{\Gamma'}{\Gamma'^2 + \Omega_\mu^2}\right) \tag{3}$$

where $\Gamma' = \gamma_2 + \omega_{\mathrm{R}}^2/\Gamma^*$.

It is readily observed from equation (3) that a dark line appear in the fluorescence spectrum when the frequency difference of the two laser radiation fields equals the hyperfine splitting of the ground state. The line-shape of the dark line is given by:

$$\pi_{\mathrm{DL}}(\Omega_\mu) = \omega_{\mathrm{R}}^2/\Gamma^* \frac{\Gamma'}{\Gamma'^2 + \Omega_\mu^2} \tag{4}$$

and its line width is:

$$\Delta\omega_{1/2} = 2\Gamma'. \tag{5}$$

The coherence term in the ground state is then given by:

$$\rho_{12} = -\frac{\omega_{\mathrm{R}}^2}{2\Gamma^*} \frac{1}{\Gamma' + \mathrm{i}\Omega_\mu} \mathrm{e}^{\mathrm{i}(\omega_1 - \omega_2)t}. \tag{6}$$

This coherence produces an oscillating magnetization at the angular frequency $(\omega_1 - \omega_2)$, as discussed in [8]. This magnetization acts as the source for a microwave field when the atomic ensemble is coupled to a microwave cavity. The power dissipated in the cavity, P_{diss}, and the emission profile of the CPT-maser are respectively:

$$P_{\mathrm{diss}} = \frac{\frac{1}{2}\hbar\,\omega_{21} k N |2\,\delta_{12}|^2}{1 + 4\,Q_{\mathrm{L}}^2 (\Delta\,\omega_{\mathrm{c}}/\omega_{21})^2}, \tag{7}$$

$$\pi_{\mathrm{M}}(\Omega_\mu) = \frac{(\omega_{\mathrm{R}}^2/\Gamma^*)^2}{\Gamma'^2 + \Omega_\mu^2}\,. \tag{8}$$

In expression (7), N is the total number of atoms coupled by the Λ scheme, Q_{L} is the quality factor of the loaded microwave cavity, $\Delta\omega_{\mathrm{c}}$ is the detuning between the cavity and the atomic line, and k may be interpreted as the number of emitted microwave photons per atom per second. The expression for k is given by [8]:

$$k = \frac{\mu_0\,\mu_{21}^2\,\eta' Q_{\mathrm{L}}\,N}{\hbar\,V_{\mathrm{a}}} \tag{9}$$

where μ_0 is the vacuum permeability, μ_{21} is the magnetic dipole moment of the transition, η' is the filling factor of the cavity and V_{a} is the volume occupied by the atomic vapor interacting with the laser field. The line width of the maser emission profile is given by (5) also in this case. According to this theory, both phenomena, dark line and maser emission, have Lorentzian shapes. We will discuss in the following paragraphs the experimental situation and the conditions which can lead to a different line-shape.

On the other hand, the intensity of the signal is proportional to $\omega_{\mathrm{R}}^2/\Gamma^*$ for the dark line, and to $(\omega_{\mathrm{R}}^2/\Gamma^*)^2$ for the CPT maser. This observation is not surprising because of the different origin of the two signals: the dark line originates from an incoherent fluorescence, while the CPT Maser signal is generated by a coherent microwave emission.

[1] In this paper we assume that the effect of microwave field on the density matrix elements is totally negligible. However, when the maser emitted power increases, the reaction of the microwave field on the atomic ensemble has to be taken into account. The solution of that case will be discussed in a future work.

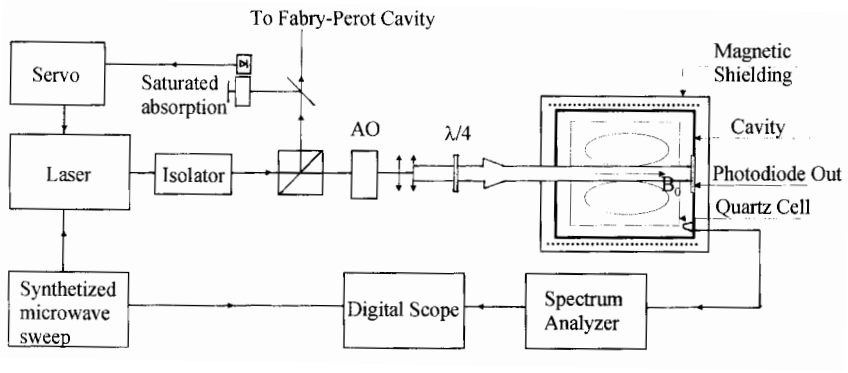

Fig. 2. Experimental set-up.

3 Experimental set-up

The experimental set-up is shown in Figure 2. Experiments have been done with the D_1 and D_2 optical transitions in the case of ^{87}Rb and with the D_2 optical transition for the case of ^{133}Cs.

The experimental set-up is made of three main parts: the optical system, the physical package and the microwave generation and detection apparatus.

The optical part provides the radiation fields necessary to excite the Λ transition: it is realized using a single laser diode, frequency modulated at half the hyperfine frequency splitting of the alkali metal atoms ground state. In that way, when the laser carrier is set to the line "center of gravity" of the transition, the first modulation sidebands are in resonance with the optical transitions. The laser center frequency is locked to a saturated absorption signal obtained with an external absorption cell, and its spectrum is monitored with a Fabry-Perot cavity used as an optical spectrum analyzer. The polarization of the beam is made circular with a $\lambda/4$ wave-plate before being sent to the microwave cavity. Consequently, the selection rules allow the excitation of only one of the possible Λ transitions (see also the next section). In the experiments, the laser intensity is approximately 200 μW/cm^2 for each sideband. An acousto-optic modulator is placed along the laser beam to act as an optical switch and to allow a precise frequency tuning with respect to the atomic optical reference, in fact, due to the presence of the buffer in the maser cell, the optical radiations are shifted with respect to the reference cell.

The physical package consists of a sealed cell inside a microwave cavity. The quartz cell containing the alkali vapor and a buffer gas (N_2 at a pressure of 19 torr for the Cs cell and 32 torr for the Rb cell) is thermally controlled. The operating temperature is around 45 °C in the case of Cs and around 60 °C in the case of rubidium. The effective cell volume is 3 cm^3 and the loaded cavity Q is 3 000 in the Cs case. In the case of Rb, the effective cell volume is 6 cm^3 and the loaded cavity Q is 10 000. The cavity used is made of brass, cylindrical, and operates in the TE_{011} mode. It is placed inside a magnetic shield package that acts also as thermal oven and a support for the C-field solenoid, a quantization field of 400 mG is applied in order

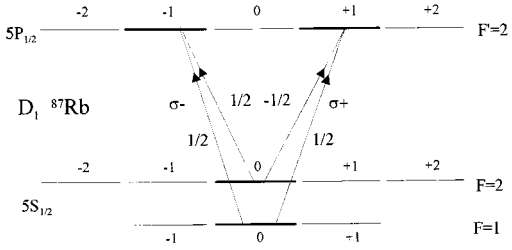

Fig. 3. Clebsch-Gordan coefficients for σ^+ and $\sigma^- - \Lambda$ transitions in ^{87}Rb D_1 line.

to resolve the Zeeman structure. A hole, covered with a layer of metal-mesh, is placed on the cavity front endcap, allowing a laser beam diameter up to 2 cm inside the maser active region without destroying the cavity quality factor.

Finally a microwave synthesizer is used to modulate the laser carrier. A high sensitivity spectrum analyzer is used as heterodyne detector. For the observation of the dark line, the experimental set-up is basically the same, but the detection is made with a photodiode by observing the laser transmission through the atomic vapor cell. The microwave cavity is absent.

4 The role of the $\lambda/4$ wave-plate

The use of a $\lambda/4$ wave-plate necessitates some explanation. In the realization of a frequency standard we are interested in the excitation of the ground $m_F = 0 \Rightarrow m_F = 0$ transition because of its low magnetic sensitivity. Since the coupling of the S ground states with $m_F = 0$ to an excited P state with $m_F = 0$ is forbidden by selection rules we are forced to use circularly polarized light and to connect the ground states to an excited $m_F = \pm 1$ state: two Λ scheme are then possible. If we look at the Clebsch-Gordan coefficients, Figure 3, we see that only one of the four coefficients that give the intensity of the two Λ transitions changes sign while the amplitude remains always the same. This means that the magnetization created with σ^+ and σ^- polarization have a different phase relation with respect to the arbitrary zero fixed by the laser modulation

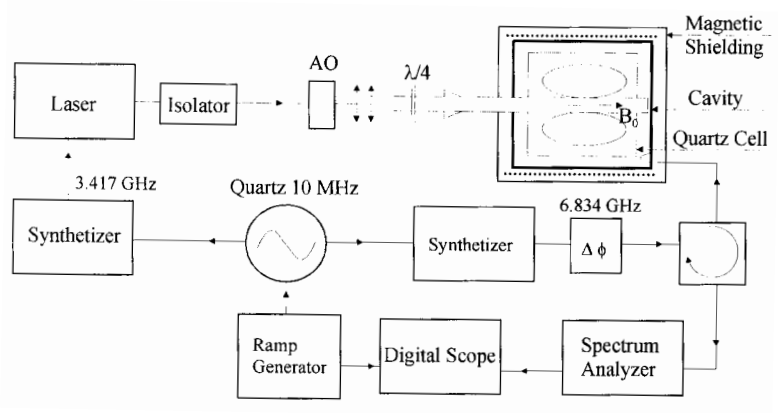

Fig. 4. Experimental set-up for the observation of the phase of the emitted microwave radiation.

phase: there is thus a phase shift equal to π between the two magnetizations.

This phase shift between the two emitted microwave radiations is experimentally confirmed. In the experimental set-up of Figure 4 two synthesizers are phase locked to a common reference, the first one is used to modulate the laser current, while the second one is used to inject a small amount of microwave power at twice the modulation frequency inside the cavity. We then detect the power generated by the sum of the two fields inside the cavity. As it is shown in Figure 5, the phase of the maser emission is shifted by π going from σ^+ to σ^-. However since the quantization axis is parallel to the light beam, it is possible in principle to use also linearly polarized light that can be thought of as a superposition of σ^+ and σ^-. It is thus possible to excite two Λ transitions, one connecting the $m_F = 0$ to $m_F = 1$ and the other one connecting $m_F = 0$ to $m_F = -1$. If this is done it is not possible to observe neither the microwave emission nor the dark line in the fluorescence spectrum, indicating that, in this case, no coherence is created in the ensemble. This means that the change in the sign of one of the Clebsh-Gordan coefficients (treated in the proper four level atomic system) inhibits the interference effects that are at the origin of the CPT phenomenon.

5 Laser Gaussian profile effect on the line-shape

It is interesting to analyze how the shapes of the dark line and of the CPT maser are modified by the laser profile used in the excitation process. These kind of effects were also studied in [9]. We assume in the following that the laser radiation has a Gaussian profile (TEM_{00} mode); the pumping rate $\omega_{\mathrm{R}}^2/\Gamma^*$ is then a function of the radial position across the laser beam. We assume moreover that the medium is optically thin and that the light absorption along the z-axis is negligible.

We can define the laser beam profile utilizing cylindrical coordinates as:

$$\omega_{\mathrm{R}}^2(\rho,\varphi,z) = \omega_{\mathrm{R}0}^2\,\mathrm{e}^{-\rho^2/\rho_0^2} \quad \forall\varphi,\ \forall z \tag{10}$$

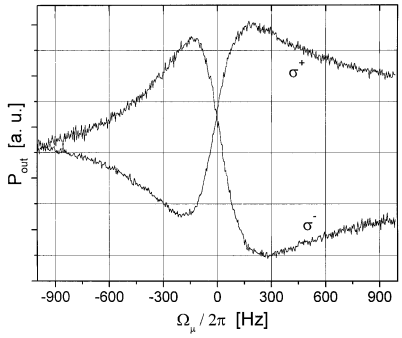

Fig. 5. Power emitted by the system in the configuration of Figure 4. Changing from σ^+ to σ^- the phase of the emitted radiation rotate by π; obviously the phase of the microwave rotates also with the span across the atomic line.

and, assuming no spatial variation along z, the line-shape can be obtained by a double integration of the profiles expressed by (4, 8) over the cylindrical coordinates ρ and φ. The new profiles are then obtained in the two cases as:

$$\begin{aligned}\Pi_{\mathrm{M}}(\Omega_\mu) &= \frac{\int_0^{2\pi}\mathrm{d}\varphi\int_0^{\infty}\rho\,\mathrm{d}\rho\,\pi_{\mathrm{M}}(\Omega_\mu)}{\int_0^{2\pi}\mathrm{d}\varphi\int_0^{\infty}\rho\,\mathrm{d}\rho\,\mathrm{e}^{-(\rho/\rho_0)^2}} \\ &= \frac{1}{2}\ln\frac{(n+1)^2+\zeta^2}{1+\zeta^2} - \frac{1}{\zeta}\arctan\frac{n\zeta}{1+n+\zeta^2}\end{aligned} \tag{11}$$

$$\begin{aligned}\Pi_{\mathrm{DL}}(\Omega_\mu) &= \frac{\int_0^{2\pi}\mathrm{d}\varphi\int_0^{\infty}\rho\,\mathrm{d}\rho\,\pi_{\mathrm{DL}}(\Omega_\mu)}{\int_0^{2\pi}\mathrm{d}\varphi\int_0^{\infty}\rho\,\mathrm{d}\rho\,\mathrm{e}^{-(\rho/\rho_0)^2}} \\ &= \frac{1}{2}\ln\frac{(n+1)^2+\zeta^2}{1+\zeta^2}\end{aligned} \tag{12}$$

where we have defined:

$$n = \frac{\omega_{\mathrm{R}0}^2}{\gamma_2\Gamma^*} \quad \text{and} \quad \zeta = \Omega_\mu/\gamma_2. \tag{13}$$

We are interested in the limit of the expressions (11, 12) in the low and high pumping rate ($n \to 0$, or $n \to \infty$).

They can be obtained as:

$$\lim_{n\to 0} \Pi_{\mathrm{DL}}(\Omega_\mu) = \frac{n}{1+\zeta^2} = \frac{\gamma_2\omega_{\mathrm{R}0}^2}{\Gamma^*}\frac{1}{\gamma_2^2+\Omega_\mu^2}, \qquad (14a)$$

$$\lim_{n\to 0} \Pi_{\mathrm{M}}(\Omega_\mu) = \frac{1}{2}\frac{n^2}{1+\zeta^2} = (\omega_{\mathrm{R}0}^2/\Gamma^*)^2\frac{1}{\gamma_2^2+\Omega_\mu^2}, \qquad (14b)$$

$$\lim_{n\to\infty} \Pi_{\mathrm{DL/M}}(\Omega_\mu) = \frac{1}{2}\ln\frac{n^2}{1+\zeta^2} = \frac{1}{2}\ln\frac{\frac{\omega_{\mathrm{R}0}^2}{\gamma_2\Gamma^*}}{1+(\Omega_\mu/\gamma_2)^2}\,. \qquad (14c)$$

The low power approximation gives again a Lorentzian shape in both cases, and the line width can always be expressed by (5). The line shape described by (14c) on the other hand is quite different from a Lorentzian shape and the line width turns out smaller than that described by equation (5) for an equivalent value of pumping rate:

$$\Delta\omega_{1/2} = 2\gamma_2\sqrt{\frac{\omega_{\mathrm{R}}^2}{\gamma_2\Gamma^*}}\,. \qquad (15)$$

The description of the experimental data with these profiles is quite satisfactory as can be seen by the fitting curves of Figure 6. In particular, in Figure 6b we report the experimental emission profile of the maser at low saturating power fitted with a Lorentzian curve; in Figure 6a the profile of the dark line observed at low saturation power is fitted with a Lorentzian curve, and in Figure 6c the emission profile of the maser excited with a high intensity laser beam is fitted with equation (14c).

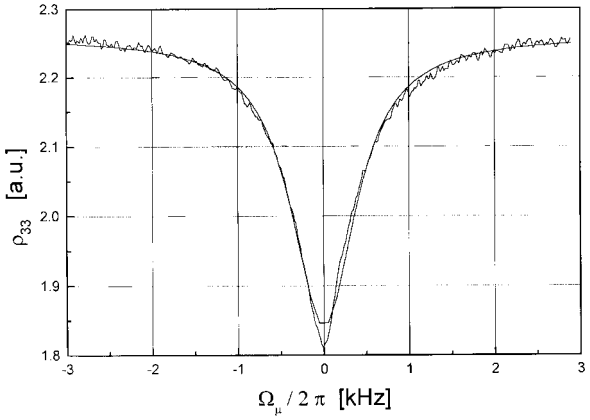

(a)

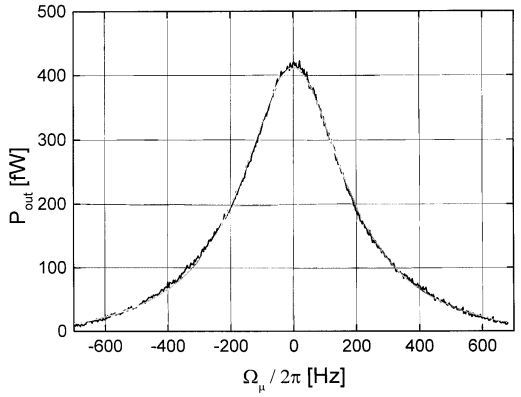

(b)

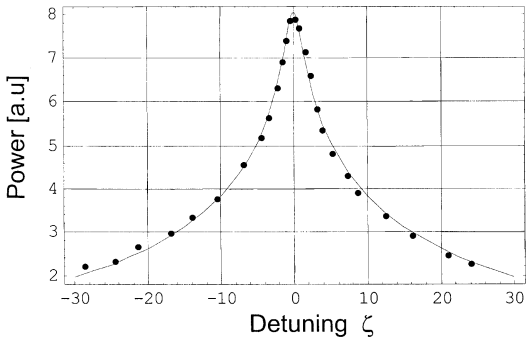

(c)

Fig. 6. (a) Dark line signal in ^{87}Rb (D_2 line): $\omega_{\mathrm{R}}^2/\Gamma^* \approx \gamma_2$ (low pumping rate). (b) Maser emission profile in ^{87}Rb (D_1 line): $\omega_{\mathrm{R}}^2/\Gamma^* \approx \gamma_2$ (low pumping rate). (c) Maser emission profile in ^{133}Cs (D_2 line): $\omega_{\mathrm{R}}^2/\Gamma^* \gg \gamma_2$ (high pumping rate).

6 Asymmetries in the excitation process

Up to now we have assumed to excite the Λ transition with a perfectly symmetric spectrum using atoms with symmetric dipole coefficients and to have a laser well tuned with respect to the atomic levels. In the following paragraphs we will investigate the effects on the atomic line-shape when these conditions are no longer respected.

It is worth noticing that since only the optical Rabi frequencies appear in the equations, it is concluded that, from the mathematical point of view, an asymmetry in the spectrum or in the Clebsch-Gordan coefficients cause similar effects. In fact, the Rabi frequency is defined as the product of the applied field time the transition dipole moment ($\omega_{\mathrm{R}1} = E_{01}\,d_{13}/\hbar$, $\omega_{\mathrm{R}2} = E_{02}\,d_{23}/\hbar$); the higher symmetry degree is one of the reasons why it is important to use the D_1 line; another reason that leads to the choice of the D_1 line is the absence of cycling transitions that could lead to strong differential absorption of the two radiation fields.

When $\omega_{\mathrm{R}1} \neq \omega_{\mathrm{R}2}$ and $\Delta_0 \neq 0$ simultaneously, it is still possible to derive an analytical solution from system (1) [9]. The solution, however, is quite complex and the mathematical expressions obtained are not transparent to a physical interpretation. A numerical integration of system (1) is best for the interpretation of the various phenomena involved. Such a calculation makes explicit two different behaviors for the dark line and the CPT maser profile. A Raman type transition that distorts the line-shape appear in the fluorescence spectrum, without moving the minimum of the profile. In the case of the maser, the emission is shifted in frequency but its line-shape

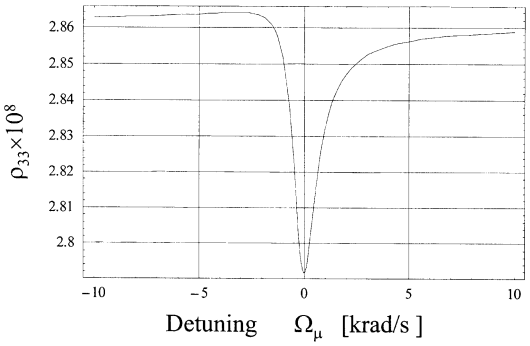

(a)

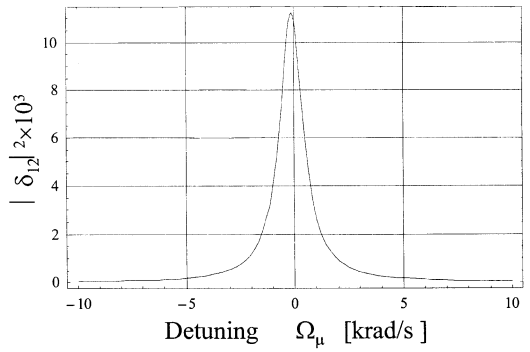

(b)

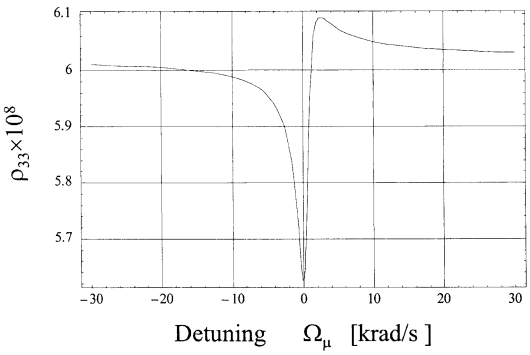

(c)

Fig. 7. (a) and (b) Calculated value of ρ_{33} and $|\delta_{12}|^2$ respectively: laser asymmetry: $\omega_{R2}/\omega_{R1} \approx 0.15$, carrier detuning 320 MHz, $\gamma_2 = 500\ s^{-1}$, $\omega_{R1}^2/\Gamma^* = 560\ s^{-1}$. (c) Calculated value of ρ_{33}: $\omega_{R1}^2/\Gamma^* = 1600\ s^{-1}$, other parameters as before specified.

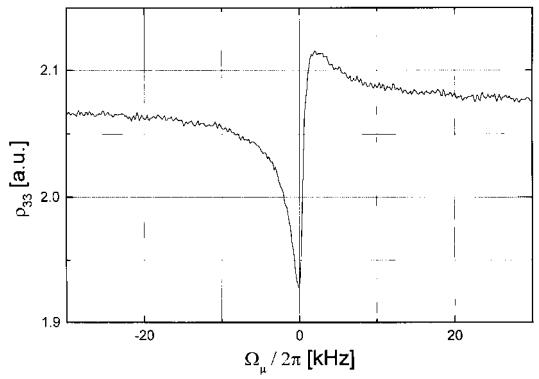

(a)

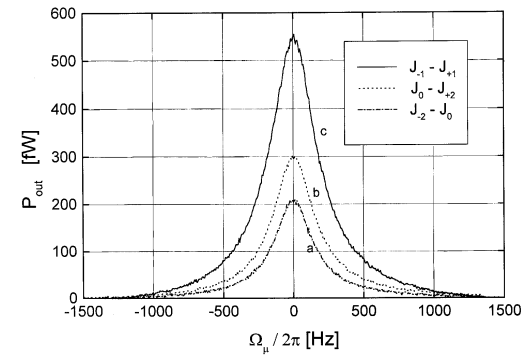

(b)

Fig. 8. (a) Dark line signal in ^{87}Rb (D_2 line): laser power $(\omega_{R1}^2/\gamma_2\Gamma^*) \approx 5$, carrier detuning 350 MHz, $\omega_{R2}/\omega_{R1} \approx 0.5$. (b) Maser emission profile in ^{87}Rb (D_1 line): $(\omega_{R1}^2/\gamma_2\Gamma^*) \approx 0.5$ in the excitation process the two first sidebands are used ($\omega_{R2}/\omega_{R1} \approx 1$) curve c, or the carrier and the second harmonic ($\omega_{R2}/\omega_{R1} \approx 0.05$), curve b and a, laser detuning 100 MHz.

is not affected by the Raman transition. This difference is due to the fact that while the CPT maser emission is a phenomenon related only to the coherence in the ground state, the dark line is observed trough the Electromagnetically Induced Transparency and is thus sensitive to all the effects that affect the excited state population.

Calculated profiles when a carrier detuning of 300 MHz is present ($\Delta_0 \approx \Gamma^*/2$) together with a laser asymmetry of 85% are reported in Figure 7. As can be seen, the maser emission profile is a Lorentzian shifted by 140 rad/s while the dark line is distorted, but the minimum of ρ_{33} remains always at $\Omega_\mu = 0$. With the same asymmetry but much higher laser power, it is possible to enhance the Raman transition, but the minimum always remains at zero detuning (Fig. 7c).

Experimental observations confirm these results with respect to the line-shapes. In order to excite the Λ transition with strongly asymmetric radiation fields, it is possible, in practice to use the carrier and the second harmonic of the modulation frequency instead of the two first sidebands. In Figure 8 some experimental profiles are reported for the dark line and for the CPT maser. The results confirm that the maser emission profile is always Lorentzian no matter what is the laser detuning and what is the laser asymmetry, while the shape of the dark line is sensitive to the parameters mentioned above.

Measurement of the shift of the CPT-Maser profile is a more complex problem. In fact, as it was discussed in [11] the total light shift (accounted for in the static Hamiltonian operator, as well as other effect like for example buffer gas and static Zeeman shifts) is a complex function of the modulation index and of the carrier detuning.

It is thus extremely difficult to distinguish between the static light shift and the dynamic light shift described above, using the present experimental set-up.

7 Conclusions

We have investigated the line-shape of the dark line and of the CPT maser emission profile observed in rubidium and in cesium vapor cells containing a buffer gas. In particular a non-Lorentzian line shape is determined by the joint effect of a Gaussian laser field profile and a high pumping rate. Moreover the imbalance of the optical Rabi frequencies in the Λ scheme together with a detuning of the laser carrier frequency with respect to the "center of gravity" of the optical transitions produces a significant asymmetry in the line-shape of the dark line and a shift of the maser emission profile. All the above mentioned effect have been theoretically explained in the framework of a three level system and, with the exception of the precise measurement of the CPT maser frequency shift for the reasons reported before, found in good agreement with the experimental results obtained on the optical transitions of ^{133}Cs (D_2 line) and ^{87}Rb (D_1 and D_2 lines).

The theory on the line-shape of the CPT maser, reported in this paper, refers to the case of a negligible feedback of the microwave cavity field on the atomic ensemble. With the removal of this hypothesis, new effects are expected which will be examined in a forthcoming paper.

We would like to thank J.C. Camparo for useful discussions, M. Inguscio for his help at different stages of the work and ASI for financial support.

References

1. A. Godone, F. Levi, J. Vanier, IEEE Trans. Instrum. Meas. **48**, 504 (1999).
2. N. Cyr, M. Têtu, M. Breton, IEEE Trans. Instrum. Meas. **42**, 640 (1993).
3. N. Vukicevic *et al.*, in *Proceedings of 1999 Joint EFTF and IEEE-IFCS meeting*, Besançon, 1999, p. 133.
4. H. Lee, M. Fleischhauer, M.O. Scully, Phys. Rev. A **58**, 2587 (1998); A. Nagel *et al.*, Europhys. Lett. **44**, 31 (1998).
5. G. Alzetta *et al.*, Nuovo Cimento B **36**, 5 (1976).
6. A. Godone, F. Levi, J. Vanier, Phys. Rev. A **59**, 1 (1999).
7. E. Arimondo, Prog. Optics **35**, 257 (1996).
8. J. Vanier, A. Godone, F. Levi, Phys. Rev. A **58**, 2345 (1998).
9. G. Orriols, Nuovo Cimento B **53**, 1 (1979).
10. P. Minguzzi *et al.*, J. Opt. Soc. Am. B **3**, 1075 (1986).
11. F. Levi, A. Godone, J. Vanier, IEEE Trans. UFFC **47**, 2 (2000).